Tripartite entanglement generation via four-wave mixings: narrowband triphoton W state

Jianming Wen,[1,*] Eun Oh,[2] and Shengwang Du[3]

[1]*Department of Physics, University of Arkansas, Fayetteville, Arkansas 72701, USA*
[2]*Remote Sensing Division, U.S. Naval Research Laboratory, Washington, D.C. 20375, USA*
[3]*Department of Physics, The Hong Kong University of Science and Technology, Clear Water Bay, Kowloon, Hong Kong, China*
**Corresponding author: jianming.wen@gmail.com*

Received August 3, 2009; revised December 13, 2009; accepted December 19, 2009; posted January 5, 2010 (Doc. ID 115050); published February 9, 2010

We propose a method to generate a narrowband triphoton W state entangled in time (or energy) via two four-wave mixing processes in cold atomic gas media. The calculation of such a triphoton W state is performed with second-order perturbation theory. To characterize the optical properties of the state, we analyze the two-photon and three-photon temporal correlations in the photon coincidence counting measurement. Considering the role of determining the time coherence of triphotons between the nonlinear susceptibilities and phase matchings, we concentrate on two regimes, damped Rabi oscillation and group delay, to look at the temporal correlations. To further enhance the nonlinear interactions, it may be promising to consider cold atoms confined within hollow fibers or loaded into a high-Q cavity. © 2010 Optical Society of America

OCIS codes: 270.0270, 190.4380, 190.4410, 030.5260.

1. INTRODUCTION

Entangled photons of $n \geq 3$ have attracted a great deal of interest because of their roles in probing the foundations of quantum theory and their potential applications in quantum information processing, quantum communication, quantum cryptography, quantum computation, quantum metrology, quantum imaging, and quantum lithography. In the past decades, experimental efforts in the realization of multiphoton entangled states have paved a new stage for the study of multipartite entanglement. In entangled three-qubit states, two classes of genuine tripartite entanglement have been known, namely, the Greenberger–Horne–Zeilinger (GHZ) class [1] and the W class [2]. The entanglement in the W state is robust against the loss of one qubit, while the GHZ state collapses down to a product of two qubits. It has been shown that these two classes are intrinsically inequivalent under stochastic local operations and classical communications [3,4].

Up to date, the polarization-entangled triphoton GHZ and W states have been well demonstrated in optical and trapped ion experiments [5–12] by using either post-selection from the spontaneous parametric downconversion (SPDC) processes or SPDC biphoton state with an attenuated coherent stated. The recent progress in continuous-variable (CV) multiparticle entanglement [13–15] promises the practical development of quantum cryptography techniques, quantum communication, and quantum information science. However, the CV analysis involves the quadrature-type measurement, which is very different from the direct photon-counting detection as shall be presented in this paper. Very recently, the distinction of triphoton GHZ and W states entangled in time and space has been reported by comparing the second-order and third-order correlation functions [16]. The results showed that the $|1,2\rangle$ state is inequivalent to the $|1,1,1\rangle$ state, where $|i,j,l\rangle$ represents i, j, and k photons with modes $\vec{k}_i$, $\vec{k}_j$, and $\vec{k}_l$, respectively, in the state. $|1,2\rangle$ behaves as a GHZ state and is fragile to the loss of photons, whereas $|1,1,1\rangle$ has properties of the W class and is resistant to photon loss. Use of these states for quantum imaging has been presented in [17,18] where achieving spatial resolution beyond the Rayleigh diffraction limit has been explored. It has been pointed out that, although one could use triphoton W state to mimic some properties of three-photon GHZ state in the imaging system, the Gaussian thin lens equations and the physics behind are quite different [16].

Narrowband entangled photons are a key ingredient of recently proposed protocols for (long-distance) quantum communication and quantum information processing based on coherent interaction between single photons and atomic ensembles [19], which requires absorbing photons efficiently and storing the entanglement. Paired entangled photons produced from SPDC in nonlinear crystals [20] are usually associated with very broad bandwidth, typically about a few terahertz, which limits their direct application to these protocols. The progress towards obtaining narrowband biphotons has been made by utilizing high-quality cavities to reduce the bandwidth of SPDC photons. A bandwidth of about 10 MHz and a coherence time of about 50 ns have been reported in the literature [21–24]. In the past few years, an alternative methodology to achieve narrowband biphotons in cold atomic gases through the process of four-wave mixing (FWM) has attracted a considerable interest from both the theoretical side [25–34] and the experimental aspect [35–38]. With the assistance of two mature techniques,

i.e., laser cooling and trapping [39] and electromagnetically induced transparency (EIT) [40,41], paired photons can be created near atomic resonance with long time coherence, high spectral brightness, and high conversion efficiency. The bandwidth of these biphotons typically ranges from tens of megahertz down to hundreds of kilohertz, which makes them ideal for atomic-ensemble-based quantum memory and quantum communication protocols.

In this paper we propose a method to generate a narrowband triphoton W state entangled in time-energy (and space) from cold atomic gas media via two FWM processes. These narrowband triphotons may have important applications in long-distance quantum communication and quantum information processing. It is worthwhile to mention that the methods to create polarization-entangled GHZ and W states [5–12] are not useful to study the temporal correlations of these triphotons, because of identical mode selection among three photons. We note that there are other ways to produce such a W state in the literature. One way is the cascade configuration in which a pump photon is downconverted into three daughter photons [42]. The other way is proposed by Keller *et al.* [43] with use of two parametric downconversions followed by one upconversion. Due to the inefficient nonlinear interaction, however, it makes these schemes impractical and experimentally challenging. Taking advantage of enhancing nonlinear interaction with EIT, our proposed scheme might be doable in current labs. Number of new features can be found in the current scheme. One feature is that almost maximal entanglement exists even in two-partite subsystems of triphotons, which gives a strong contrast with polarization-entangled W state where only partial entanglement can be achieved in two-partite subsystems. This property is of importance for the application where photon loss is a severe issue. Another feature is that by manipulating the EIT slow-light effect, triphotons with subnatural linewidth can be achieved in analogy with the paired photons case [38]. The long coherence time obtained here offers a way to (arbitrarily) shape triphoton waveform, which is useful for quantum information processing. To further improve the nonlinearity and confine the photons, either hollow fibers doped with cold atoms [44] or high-Q cavities loaded with cold atoms [45] may offer an excellent environment for these studies.

We shall model the generated three-photon state by using second-order perturbation theory. We find that the optical properties of such a triphoton state are determined by both the nonlinear susceptibilities and phase-matching conditions. Alternatively, the time coherence of these triphotons is governed by both the third-order nonlinear susceptibilities and the phase matchings, similar to biphoton generation [25,27–29,32]. This method provides a way to look at the physics in different regimes by noticing which one is dominant in controlling the temporal coherence between nonlinear susceptibilities and phase matchings. We therefore focus on two simple cases, damped Rabi oscillation regime and group-delay regime, which yields insights into the process of triphoton generation. Our results show that in the damped Rabi oscillation region, the feature of damped Rabi oscillations in two FWM processes has been imprinted into the three-photon coincidence counts. The conditional three-photon coincidence counts reveals the same curvature as the two-photon coincidences. In the group-delay regime, we find that the mechanism of triphoton generation is washed out by the longer coherence time due to the phase matchings. In such a case, the pattern of conditional three-photon and two-photon coincidence counting rates is a (decayed) square wave similar to that observed in the conventional SPDC photons. The frequencies created out of the phase matching may yield the three-photon precursor phenomenon. For simplicity, we focus here on the temporal behavior of triphotons and ignore the transverse correlations, which may be useful for quantum imaging and lithography. The transverse effects can be analyzed by following the treatments presented in [17,18,25,26]. To simplify the discussion, the atoms are assumed to be laser cooled, and therefore Doppler effects can be neglected. Since we are interested in coincidence counting, nonpaired photons will not contribute to the correlation measurement and can be ignored for simplicity. Other degrees of freedom of photons (e.g., polarizations) are not the focus of this paper and will not be specified here either.

The paper is organized as follows. In Section 2, we describe the triphoton W state generated from two FWM processes using second-order perturbation theory. To characterize optical properties of the temporal correlation, in Section 3 we evaluate the second-order and third-order correlation function in photon-counting measurements. We concentrate on two regimes, damped Rabi oscillation and group delay, to discuss the two-photon and three-photon coincidence counts. Finally, we draw our conclusion in Section 4.

2. GENERATION OF TRIPHOTON W STATE

We illustrate the basic idea of generating a three-photon W state in Fig. 1(a), where three input beams, one pump (E_p) and two controls (E_{c1} and E_{c2}), are assumed to be monochromatic plane waves, and their angular frequencies and wave numbers are (ω_p,k_p), (ω_{c1},k_{c1}), and

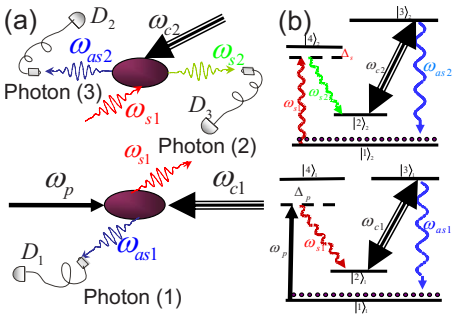

Fig. 1. (Color online) Generation of a triphoton W state entangled in time-energy (and space). (a) Schematic of triphoton W state generation and detection in the backward geometry. Two counterpropagating weak pump field (ω_p) and strong control field (ω_{c1}) induce spontaneous emission of paired Stokes (ω_{s1}) and anti-Stokes (ω_{as1}) photons in the first atomic ensemble. By sending the ω_{s1} photon with another strong control laser (ω_{c2}) into the second ensemble, another paired Stokes (ω_{s2}) and anti-Stokes (ω_{as2}) photons are created. This completes the three-photon state formation. (b) Four-level double-Λ EIT configurations for triphoton generation.

(ω_{c2},k_{c2}), respectively. As illustrated in Fig. 1(a), the first FWM offers a pair of entangled Stokes and anti-Stokes photons (E_{s1},E_{as1}) by absorbing one input ω_p pump and one ω_{c1} control photon. By sending the Stokes photon (E_{s1}) produced from the first FWM as a pump field to trigger the second FWM, another pair of entangled Stokes (E_{s2}) and anti-Stokes (E_{as2}) photons is initiated from the second atomic ensemble by annihilating simultaneously the input Stokes photon (E_{s1}) and one control photon (E_{c2}). This completes the three-photon state generation. The angular frequencies and wave vectors associated with the generated weak fields are represented by $(\omega_j,\vec{k}_j)$ with the subscript j running among $(s1,as1,s2,as2)$. We will use (ϖ_j,K_j) to stand for the central angular frequency and central wave number of the generated field. The atomic-level configurations under consideration are, for simplicity, taken as two four-level double-Λ EIT systems as shown in Fig. 1(b). We also assume that all the population in both systems are initially distributed in the ground state $|1\rangle_j$ where the subscript $(j=1,2)$ represents two ensembles. The input weak pump and Stokes field are tuned to the atomic transition $|1\rangle_j \rightarrow |4\rangle_j$ with detunings $\Delta_p=\omega_p-\omega_{41,1}$ and $\Delta_s=\omega_s-\omega_{41,2}$, where $\omega_{41,j}$ is the corresponding transition frequency of the jth medium. Two control lasers (E_{c1},E_{c2}) are tuned resonant with their corresponding atomic transitions. Three single-photon detectors are arranged that detector D_1 detects the ω_{as1} photons, D_2 collects the ω_{as2} photons, and D_3 fires the ω_{s2} photons. For simplicity, we will focus on the counterpropagating geometry in the photon-counting measurement (see Fig. 1(a)). One advantage of this experimental configuration is that, in such a scheme, the input and output beams can be easily separated.

To calculate the three-photon state at the output surfaces of the media, we shall work in the interaction picture and start with the effective interaction Hamiltonians [25,32], which are

$$H_1(t_1)=\int_{V_1} d^3r\varepsilon_0\chi_1^{(3)}E_p^{(+)}E_{c1}^{(+)}E_{s1}^{(-)}E_{as1}^{(-)}+H.c.,$$

$$H_2(t_2)=\int_{V_2} d^3r\varepsilon_0\chi_2^{(3)}E_{s1}^{(+)}E_{c2}^{(+)}E_{s2}^{(-)}E_{as2}^{(-)}+H.c., \quad (1)$$

where the integrals are performed over the interaction volume (V_j) of the medium illuminated by two input fields, $\chi_j^{(3)}(j=1,2)$ is the third-order nonlinear susceptibility, and H.c. means the Hermitian conjugate. The electric fields of the generated beams for Stokes and anti-Stokes $(j=s1,as1,s2,as2)$ are described by the quantized fields

$$E_j^{(+)}=\sum_{\vec{k}} E_j a(\vec{k}_j)e^{i(\vec{k}_j\cdot\vec{r}-\omega_j t)}, \quad (2)$$

where $a(\vec{k}_j)$ is the annihilation operator for the mode with wave vector $\vec{k}_j$ and angular frequency ω_j. The dispersion relation inside the medium is $|\vec{k}_j|=\omega_j n_j/c=k_j$, n_j is the index of refraction,

$$E_j=i\sqrt{\frac{\hbar\omega_j}{2\varepsilon_0 n_j^2 V_q}}, \quad (3)$$

and V_q is the quantization volume. The creation and annihilation operators are normalized so that the common commutation relationship is satisfied:

$$[a(\vec{k}_j),a^\dagger(\vec{k}_l)]=\delta_{\vec{k}_j\vec{k}_l}. \quad (4)$$

We take three input beams, one weak pump (E_p), and two strong control $(E_{c1,c2})$ fields, to be classical plane waves:

$$E_p^{(+)}=E_p e^{i(k_p z-\omega_p t_1)}, \quad E_{cj}^{(+)}=E_{cj}e^{-i(k_{cj}z+\omega_{cj}t_j)}, \quad (5)$$

where E_j is the strength of the field amplitude, and the $+z$ direction is assumed to be pointed along the propagation direction of the input ω_p (or ω_{s1}) beam.

The state vector of triphotons generated from the scheme shown in Fig. 1 can be derived from second-order perturbation theory. That is,

$$|\Psi\rangle=\left(-\frac{i}{\hbar}\right)^2\int_{-\infty}^{\infty}dt_2\int_{-\infty}^{\infty}dt_1\mathcal{T}[H_2(t_2)H_1(t_1)]|0\rangle, \quad (6)$$

where $\mathcal{T}$ is the time-ordering operator and $|0\rangle$ is the initial vacuum state. By using Eqs. (1)–(6) and keeping only the terms of interest, the triphoton state vector (6) becomes

$$|\Psi\rangle=\sum_{\vec{k}_{as1}}\sum_{\vec{k}_{s2}}\sum_{\vec{k}_{as2}}F(\vec{k}_{as1},\vec{k}_{s2},\vec{k}_{as2})a^\dagger(\vec{k}_{as1})a^\dagger(\vec{k}_{s2})a^\dagger(\vec{k}_{as2})|0\rangle, \quad (7)$$

where the three-photon spectral function F is given by

$$F(\vec{k}_{as1},\vec{k}_{s2},\vec{k}_{as2})=\sum_{\vec{k}_{s1}}\beta\chi_1^{(3)}\chi_2^{(3)}\Phi_1(\Delta k_1L_1)\Phi_2(\Delta k_2L_2)H_{tr1}(\vec{\alpha}_{s1}+\vec{\alpha}_{as1})H_{tr2}(\vec{\alpha}_{s1}-\vec{\alpha}_{as2}-\vec{\alpha}_{s2})\times\delta(\omega_p+\omega_{c1}-\omega_{s1}-\omega_{as1})\delta(\omega_{s1}+\omega_{c2}-\omega_{s2}-\omega_{as2}). \quad (8)$$

In Eq. (8), two Dirac δ functions come from time integrals in the steady-state approximation, and physically they assure the energy conservation in the processes. From the point view of atomic populations, the energy conservations indicate that after completing the generation processes, the populations return to their initial conditions. $\Phi_j(\Delta k_jL_j)$ $(j=1,2)$ is called the longitudinal detuning function:

$$\Phi_j(\Delta k_jL_j)=\frac{1-e^{-i\Delta k_jL_j}}{i\Delta k_jL_j}=\mathrm{sinc}\left(\frac{\Delta k_jL_j}{2}\right)e^{-i\Delta k_jL_j/2}, \quad (9)$$

and is the z integration from $-L_j$ to 0 over the length of the medium. Here $\Delta k_1=k_p-k_{c1}-k_{s1}+k_{as1}$ and $\Delta k_2=k_{s1}-k_{c2}-k_{s2}+k_{as2}$ are the phase mismatchings along the longitudinal direction, and their forms will be specifically evaluated below. The natural spectral width of the triphoton wave packet is determined by these longitudinal functions. Accordingly, H_{trj} $(j=1,2)$ is called the transverse detuning function and is defined by

$$H_{tr1}(\vec{\alpha}_{s1}+\vec{\alpha}_{as1})=\frac{1}{A_1}\int_{A_1}d^2\rho e^{-i(\vec{\alpha}_{s1}+\vec{\alpha}_{as1})\cdot\vec{\rho}},$$

$$H_{tr2}(\vec{\alpha}_{s1}-\vec{\alpha}_{s2}-\vec{\alpha}_{as2})=\frac{1}{A_2}\int_{A_2} d^2\rho e^{i(\vec{\alpha}_{s1}-\vec{\alpha}_{s2}-\vec{\alpha}_{as2})\cdot\vec{\rho}}. \quad (10)$$

In the derivations of Eq. (10), the cross section area A_j independent of z is assumed. $\vec{\alpha}_j$ is the transverse wave vector of the generated field ($j=s1,as1,s2,as2$). $\vec{\rho}$ is sitting in the transverse plane perpendicular to the longitudinal axis z. $\xi=\beta\chi_1^{(3)}\chi_2^{(3)}$ is the so-called parametric gain index and

$$\beta=-i\pi^2E_{c1}E_{c2}E_p\frac{\varpi_{s1}\sqrt{\varpi_{s2}\varpi_{as2}}}{n_{s1}^2n_{s2}n_{as2}}\sqrt{\frac{\hbar\varpi_{as1}}{2\varepsilon_0n_{as1}^2V_q}}. \quad (11)$$

For the atomic gas media discussed here, the indices of refraction are almost unity and, therefore, we will take all $n_j=1$ from now on. From the expression of Eq. (11) we see that to obtain a higher triphoton generation rate, it is critical to achieve a larger single-photon electric field in the second medium. This may be achievable using hollow fibers to confine the cold atoms or loading cold atoms into a high-Q cavity. The parametric gain ξ is generally frequency-dependent because of $\chi_j^{(3)}$. If $\chi_j^{(3)}$ varies smoothly within the range of allowable frequencies, they may be pulled out of the integrals and treated as a constant as routinely done in biphoton generation using nonlinear crystals (e.g., BBO crystals) [46–48].

As seen from Eqs. (7) and (8), the three-photon state is entangled in frequency and wave number but is not entangled in polarization. In frequency space, the entanglement is the result of the frequency phase-matching condition, which implies that detections of two photons at frequencies ω_{as1} and ω_{as2} require the detection of the third one at frequency $\omega_p+\omega_{c1}+\omega_{c2}-\omega_{as1}-\omega_{as2}$. The frequency correlation has interesting consequences for the temporal behavior of the tripartite system, as we shall study in the following section.

From Eq. (8), it is obvious that Φ_j's and H_{trj}'s become δ functions in the limit of the media with infinite length and cross sectional area. Plus the energy conservation δ functions, they together form perfect phase-matching conditions:

$$\omega_p+\omega_{c1}=\omega_{s1}+\omega_{as1},\quad \omega_{s1}+\omega_{c2}=\omega_{s2}+\omega_{as2},$$

$$k_p-k_{c1}=\vec{k}_{s1}-\vec{k}_{as1},\quad \vec{k}_{s1}-k_{c2}=\vec{k}_{s2}-\vec{k}_{as2}.$$

The natural spectral width of the triphoton wave packet is usually controlled by the longitudinal detuning functions, Φ_j, through manipulating the light propagations inside the materials. Before proceeding, it is instructive to look at the phase mismatching in the longitudinal axis. We first approximate the frequencies as small deviations around the corresponding central frequencies, i.e., $\omega_{asj}=\varpi_{asj}+\nu_j$ ($j=1,2$), where the range of frequencies reaching each detector, ν_j, is limited so that $|\nu_j|\ll\varpi_{asj}$. From the energy conservation, automatically we have $\omega_{s2}=\varpi_{s2}-\nu_1-\nu_2$. We then expand the wave numbers to first order, i.e., $k_{asj}=K_{asj}+\nu_j/v_{asj}$, where v_{asj} is the group velocity of the anti-Stokes ω_{asj} photon traversing through the jth ensemble. To maximize the output efficiency of the interaction, we arrange the system to satisfy, for $j=1,2$:

$$K_{s1}-K_{as1}=k_p-k_{c1},\quad K_{s2}-K_{as2}=K_{s1}-k_{c2},$$

$$\varpi_{s1}+\varpi_{as1}=\omega_p+\omega_{c1},\quad \varpi_{s2}+\varpi_{as2}=\varpi_{s1}+\omega_{c2}. \quad (12)$$

With these approximations the phase mismatching Δk_j can be evaluated as

$$\Delta k_1=\nu_1\left(\frac{1}{v_{s1}^{(1)}}+\frac{1}{v_{as1}}\right),$$

$$\Delta k_2=\nu_1\left(\frac{1}{v_{s2}}-\frac{1}{v_{s1}^{(2)}}\right)+\nu_2\left(\frac{1}{v_{s2}}+\frac{1}{v_{as2}}\right), \quad (13)$$

where $v_{s1}^{(j)}$ is the group velocity of the Stokes (ω_{s1}) photon propagating in the jth atomic ensemble, and v_{s2} is the group velocity of the ω_{s2} photon. It is known that in the four-level double-Λ EIT system, because of far-detuning for input pump (and Stokes) field only the anti-Stokes photons experience ultraslow light effect [32,35], and other electromagnetic fields propagate at almost the speed of light in vacuum. Equation (13) hence simplifies as

$$\Delta k_1=\frac{\nu_1}{v_{as1}},\quad \Delta k_2=\frac{\nu_2}{v_{as2}}. \quad (14)$$

This simplification has an important influence to the optical property of triphotons discussed here. It results in the conditional three-photon coincidence counting rate sharing the same functional shape with the two-photon coincidence counting rate in the group-delay regime (see the next section). This is different from the nonlinear crystal case, where the difference between the group velocities associated with photons is relatively small so that one has to take into account all the group velocities [16,43].

The transverse properties of triphotons are governed by the transverse detuning functions, H_{trj}. The transverse correlation of entangled photons has practical applications in quantum imaging, quantum lithography, and quantum sensors. In this paper, the temporal correlation of entangled photons is of our primary interest and we will ignore the spatial effects. The transverse effects of the generated triphotons proposed here can be examined by following the analysis presented in [17,18,25,33]. By assuming that the intersections between the input beams are large enough, we can approximate the transverse detuning functions, H_{trj}, as Dirac δ functions and accordingly replace the wave vectors by the wave numbers. From Eqs. (7) and (8) we also notice that the state property and the spectral function are characterized by both the nonlinear susceptibilities and the phase-matching conditions. As a consequence, this plays a major role in the temporal correlation as shall be discussed in the following section.

3. TEMPORAL CORRELATION OF TRIPHOTONS

Optical properties of triphotons are revealed by studying the photon statistics in the photon-counting measurement. In this section, we will study the temporal correla-

tion by analyzing the second-order and third-order correlation functions. In Ref. [16] the distinction between GHZ and W three-photon states was demonstrated by comparing the second-order $[G^{(2)}]$ with third-order $[G^{(3)}]$ coherence functions. It is proven that a partial entanglement can, indeed, exist between two particles in triphoton W state $|1,1,1\rangle$, which indicates the robustness against loss of one particle. Hence here we shall examine the two-photon coincidence counts and three-photon coincidence counts. We assume that the ω_{as1} photon goes to detector D_1, the ω_{s2} goes to detector D_2, and the ω_{as2} to D_3, as shown in Fig. 1(a). Again, we will ignore the polarization property of the generated weak fields.

Using Glauber's theory, the averaged triphoton coincidence counting rate is

$$R_3 = \lim_{T\to\infty}\frac{1}{T}\int_0^T dt_1\int_0^T dt_2\int_0^T dt_3\langle\Psi|E_1^{(-)}(\tau_1)E_2^{(-)}(\tau_2)E_3^{(-)} \times(\tau_3)E_3^{(+)}(\tau_3)E_2^{(+)}(\tau_2)E_1^{(+)}(\tau_1)|\Psi\rangle, \tag{15}$$

and the two-photon coincidence counting rate is

$$R_2 = \lim_{T\to\infty}\frac{1}{T}\int_0^T dt_1\int_0^T dt_2\langle\Psi|E_1^{(-)}(\tau_1)E_2^{(-)}(\tau_2)E_2^{(+)}(\tau_2) \times E_1^{(+)}(\tau_1)|\Psi\rangle, \tag{16}$$

and the singles counting rate is given by

$$R_1 = \lim_{T\to\infty}\frac{1}{T}\int_0^T dt_1\langle\Psi|E_1^{(-)}(\tau_1)E_1^{(+)}(\tau_1)|\Psi\rangle. \tag{17}$$

Here $E_j^{(+)}$ $(j=1,2,3)$ is the positive frequency part of the free-space electromagnetic field evaluated at the jth detector's spatial coordinate r_j and trigger time t_j, and $\tau_j = t_j - r_j/c$, respectively. For simplicity, we shall take all single-photon detectors' efficiencies to be 100%. In this paper we are interested in narrowband triphoton generation, and the bandwidth of these triphotons is comparable with or even smaller than the spectral width of single-photon detectors used in current labs. Therefore, the three-photon coincidence counting rate (15) can be further simplified as

$$R_3 = |\langle 0|E_3^{(+)}(\tau_3)E_2^{(+)}(\tau_2)E_1^{(+)}(\tau_1)|\Psi\rangle|^2 = |A_3(\tau_1,\tau_2,\tau_3)|^2. \tag{18}$$

$A_3(\tau)$ is usually referred to as the three-photon amplitude or as the triphoton wave packet. Similarly, the two-photon coincidence counting rate (16) becomes

$$R_2 = \sum_{\vec{k}_3}|\langle 0|a(\vec{k}_3)E_2^{(+)}(\tau_2)E_1^{(+)}(\tau_1)|\Psi\rangle|^2 = \sum_{\vec{k}_3}|A_2(\tau_1,\tau_2)|^2. \tag{19}$$

The singles counting rate (17) may be written as

$$R_1 = \sum_{\vec{k}_2}\sum_{\vec{k}_3}|\langle 0|a(\vec{k}_3)a(\vec{k}_2)E_1^{(+)}|\Psi\rangle|^2 = \sum_{\vec{k}_2}\sum_{\vec{k}_3}|A_1|^2. \tag{20}$$

From Eq. (20) it is easy to see that the singles counts are not a function of time. So, we will concentrate on the two-photon and three-photon coincidences. It is worthwhile to emphasize that $A_2(\tau)$ and $A_1(\tau)$ are also the three-photon amplitudes, although some subsystems are not detected in the experiment.

Without taking into account filters inserted before detectors, plugging Eq. (7) into (18) thus yields

$$A_3(\tau_1,\tau_2,\tau_3) = A_{30}\sum_{k_{as1}}\sum_{k_{as2}}\sum_{k_{s2}} e^{-i(\omega_{as1}\tau_1+\omega_{as2}\tau_2+\omega_{s2}\tau_3)}F(k_{as1},k_{s2},k_{as2}), \tag{21}$$

where all slowly varying terms and constants have been absorbed into A_{30}. Next, we consider the two- photon coincidences with use of the triphoton entangled state (7). As an example, we examine the case that only the ω_{s2} and ω_{s2} photons are detected while the ω_{as1} remains undetected. Other possible arrangements can be calculated following the same reasoning. By substituting Eq. (7) into (19), we have

$$A_2(\tau_2,\tau_3) = A_{20}\sum_{k_{s2}}\sum_{k_{as2}} e^{-i(\omega_{as2}\tau_2+\omega_{s2}\tau_3)}F(k_{as1},k_{as2},k_{s2}), \tag{22}$$

where we have grouped all the slowly varying terms and constants into A_{20}. In addition, we have replaced the wave vectors by wave numbers in Eqs. (21) and (22). To evaluate the Dirac δ functions in the spectral function $F(k_{as1},k_{as2},k_{s2})$, a summation over a wave number will be converted into an angular frequency integral as usual:

$$\sum_{k_j}\to\frac{V_q^{1/3}}{2\pi}\int d\omega_j\frac{dk_j}{d\omega_j} = \frac{V_q^{1/3}}{2\pi}\int\frac{d\omega_j}{v_j}. \tag{23}$$

A. Two-Photon Coincidences

We start with the two-photon temporal correlation using the triphoton state given in Eq. (7). We continue examining our example mentioned above [see Eq. (19) or Eq. (22)]. With use of Eqs. (7), (19), (22), and (23), after some algebra it is not difficult to show that the two-photon coincidence counting rate is

$$R_2(\tau_{23}) = R_{20}\int d\nu_1\left|\chi_1^{(3)}(\nu_1)\mathrm{sinc}\left(\frac{\nu_1 L_1}{2v_{as1}}\right)\right|^2\left|\int d\nu_2\chi_2^{(3)} \times(\nu_1,\nu_2)\mathrm{sinc}\left(\frac{\nu_2 L_2}{2v_{as2}}\right)e^{-i\nu_2(\tau_{23}+L_2/2v_{as2})}\right|^2, \tag{24}$$

where $\tau_{23}=\tau_2-\tau_3$ and R_{20} is a grouped constant. As seen from Eq. (24), $R_2(\tau_{23})$ is a function of τ_{23}, which means a partial entanglement even between two particles in such a triphoton state. This is clearly a signature of the property of the tripartite W class. In Eq. (24), the first integral gives a constant while the second integral inside the module is a convolution between the nonlinear susceptibility $\chi_2^{(3)}$ and the longitudinal detuning function Φ_2, which takes the same format as the case for paired photon generation in atomic gases [25,27–29,32]. The functional shape of R_2 is generally determined by both $\chi_2^{(3)}$ and Φ_2. The width of partial temporal coherence is consequently governed by the linewidths of resonances appearing in

$\chi_2^{(3)}$ and the natural spectral width from Φ_2. Therefore, in the following we will look at $R_2(\tau_{23})$ in two cases: damped Rabi oscillation regime and group-delay regime.

1. Damped Rabi Oscillation Regime

In the damped Rabi oscillation regime, the temporal coherence of triphotons is mainly determined inversely by the linewidths of resonances appearing in nonlinear susceptibilities. In such a limit, the temporal coherence resulting from the phase matchings is relatively so short that it would not be observed in the photon-counting measurement. Reaching this regime requires a medium with small optical depth such that phase matching does not play an appreciable role. The two-photon coincidence counting rate (24) now becomes

$$R_2(\tau_{23}) = R_{20}\int d\nu_1 |\chi_1^{(3)}(\nu_1)|^2 \left| \int d\nu_2 \chi_2^{(3)}(\nu_1,\nu_2) e^{-i\nu_2\tau_{23}} \right|^2. \tag{25}$$

It is obvious that the second integral is a Fourier transform of $\chi_2^{(3)}$. The pattern of $R_2(\tau_2)$ depends on the exact form of $\chi_2^{(3)}(\nu_1,\nu_2)$.

Optical response of a four-level double-Λ EIT system have been extensively studied over the past 15 years [32,25,49,41]. For the configuration we discussed here, the third-order nonlinear susceptibilities for the first and second atomic ensembles, $\chi_1^{(3)}$ and $\chi_2^{(3)}$, are, respectively,

$$\chi_1^{(3)}(\nu_1) = -\frac{N_1\mu_{13}\mu_{32}\mu_{24}\mu_{41}}{4\hbar^3\varepsilon_0(\Delta_p + i\gamma_{14})(\nu_1 - \Omega_{e1}/2 + i\gamma_{e1})(\nu_1 + \Omega_{e1}/2 + i\gamma_{e1})}, \tag{26}$$

$$\chi_2^{(3)}(\nu_1,\nu_2) = -\frac{N_2\xi_{31}\xi_{23}\xi_{42}\xi_{14}}{4\hbar^3\varepsilon_0(\Delta_s - i\zeta_{14})(\nu_2 - \Omega_{e2}/2 + i\gamma_{e2})(\nu_2 + \Omega_{e2}/2 + i\gamma_{e2})}. \tag{27}$$

Here N_j is the atomic density of the jth ensemble, μ_{ij} and ξ_{ij} are the elements of dipole transition matrices, and γ_{14} and ζ_{14} are dephasing rates. $\Delta_s = \varpi_{s1} - \nu_1 - \omega_{41,2}$ is the input Stokes detuning from the transition $|1\rangle_2 \rightarrow |4\rangle_2$ of the second medium. $\nu_1 = \omega_{as1} - \omega_{31,1}$ is the detuning of the anti-Stokes (ω_{as1}) photons from the transition $|1\rangle_1 \rightarrow |3\rangle_1$, and we take $\varpi_{as1} = \omega_{31,1}$ as the anti-Stokes central frequency; similarly, $\nu_2 = \omega_{as2} - \omega_{31,2}$ is the detuning of the ω_{as2} photons from the transition $|1\rangle_2 \rightarrow |3\rangle_2$, and we take $\varpi_{as2} = \omega_{31,2}$ as their central frequency. $\Omega_{ej} = \sqrt{|\Omega_{cj}|^2 - (\gamma_{13,j} - \gamma_{12,j})^2}$ $(j=1,2)$ is the effective control Rabi frequency, where Ω_{cj} is the Rabi frequency of the ω_{cj} control beam, $\gamma_{13,j}$ and $\gamma_{12,j}$ are dephasing rates of coherence $|1\rangle_j \leftrightarrow |3\rangle_j$ and $|1\rangle_j \leftrightarrow |2\rangle_j$. $\gamma_{ej} = (\gamma_{13,j} + \gamma_{12,j})/2$ is the effective dephasing rate or the linewidth of the resonances appearing in $\chi^{(3)}$. This quantity sets a limit for the bandwidth of temporal coherence of entangled photons in the generation mechanism. The physics of Eqs. (26) and (27) has been fully probed in [25,27–29,32], and we will not repeat here. Interested readers please resort to those references for details.

With the help of Eqs. (25) and (27), it is easy to show that

$$R_2(\tau_{23}) = R_{20}e^{-2\gamma_{e2}\tau_{23}}[1 - \cos(\Omega_{e2}\tau_{23})]\Theta(\tau_{23}). \tag{28}$$

Again, R_{20} has absorbed all the constants and slowly varying terms. The heaviside step function $\Theta(\tau_{23})$ is defined as $\Theta(\tau_{23}) = 1$ for $\tau_{23} \geq 0$, and $\Theta(\tau_{23}) = 0$ for $\tau_{23} < 0$. One may notice that Eq. (28) has the same feature except the constant term as the biphoton generation case [see Eq. (26) in [32]]. The physics therefore holds the same interpretation as for the paired photon generation case, and it shows the beating (or interference) between two types of FWM processes occurring in the second atomic system. The two-photon temporal correlation (28) exhibits damped Rabi oscillations of period $2\pi/\Omega_{e2}$. The damping rate is determined by the resonant linewidth $2\gamma_{e2}$ in the doublet. At $\tau_{23} = 0$, R_2 vanishes and as $\tau_{23} \rightarrow \infty$, R_2 also approaches zero. This indicates the photon anti-bunching-like effect. If $\gamma_{e2} > \Omega_{e2}$, only the first oscillation is observable and the other oscillations disappear due to the fast dephasing rate γ_{e2} [35]. This can be denoted as overdamped Rabi oscillation region. Equation (28) thus proves the existence of partial entanglement in two subsystems. It is interesting to note that the width of time coherence coincides well with the width of the conditional three-photon coincidences, which shall be discussed thoroughly below. The reason is that we assume far detuning for the input ω_{s1} field. This far detuning eliminates the effect of ν_1 shown in Eq. (27) and decouples the second FWM process from the first FWM influence. In the counterpropagation geometry, R_2 may become a symmetric distribution about $\tau_{23} = 0$ if $\vec{k}_{s1} + \vec{k}_{c2} = 0$ is satisfied, because spontaneously emitted ω_{s2} and ω_{as2} photons can trigger both detectors D_2 and D_3 [36]. In Fig. 2(a) and 2(b) we have simulated R_2 as a function of τ_{23} in both damped and overdamped Rabi oscillation regimes.

2. Group-Delay Regime

The group-delay regime is defined as the time coherence from phase matching being greater than the time coherence from the nonlinear susceptibility. Alternatively, the third-order nonlinear susceptibilities can be treated as constants over the phase-matching spectrum. As a consequence, the mechanism of paired photon generation in FWMs is erased by the longer group-delay time [37]. In the group-delay regime, the triphoton temporal coherence can be controlled by dynamically manipulating the (EIT) slow-light effect. To experimentally observe the feature in such a region, it is necessary to trap the atoms with high optical depth (OD) so that the slow light is dominant in the system. The two-photon correlation in this regime is closer to the correlation with conventional SPDC photons.

The two-photon coincidence counting rate (24) now reads

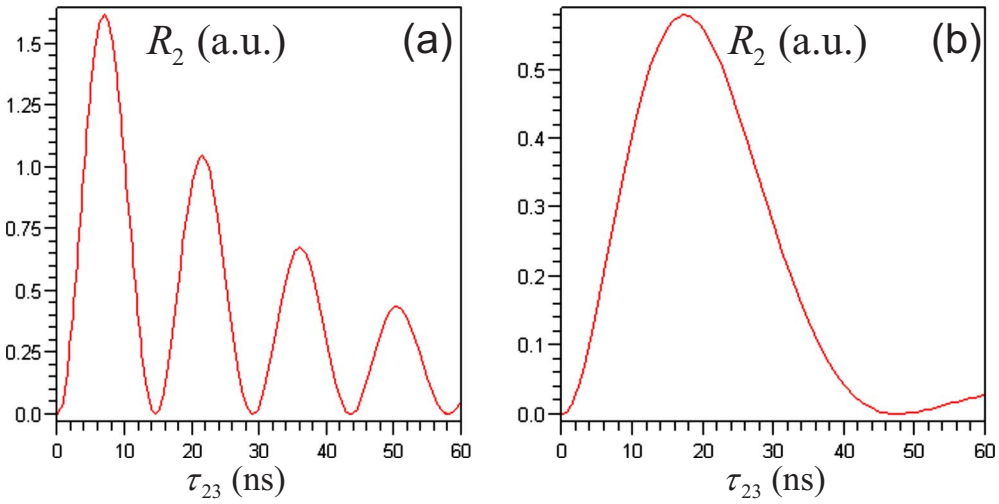

Fig. 2. (Color online) Two-photon coincidences in the damped (a) and overdamped Rabi oscillation regions. The parameters are chosen as in (a) $\gamma_{31}=6\pi$ MHz, $\gamma_{21}=0.6\gamma_{31}$, $\Omega_{c1}=23\gamma_{31}$; and (b) $\Omega_{c1}=7\gamma_{31}$.

$$R_2(\tau_{23}) = R_{20}\int d\nu_1 \left|\mathrm{sinc}\left(\frac{\nu_1 L_1}{2v_{as1}}\right)\right|^2 \left|\int d\nu_2 \times \mathrm{sinc}\left(\frac{\nu_2 L_2}{2v_{as2}}\right) e^{-i\nu_2(\tau_{23}+L_2/2v_{as2})}\right|^2. \quad (29)$$

The second integral in Eq. (29) is a Fourier transform of the sinc function. Same as SPDC [46,50], this integral yields a square wave with width L_2/v_{as2}. By manipulating the ODs and the Rabi frequencies of the $E_{c1,c2}$ fields, as the EIT bandwidth ($\Delta\omega_{\mathrm{EIT},j}\simeq|\Omega_{cj}|^2/(2\gamma_{13,j}\sqrt{\mathrm{OD}})$) is larger than the phase-matching bandwidth, the anti-Stokes loss can be ignored and the two-photon wave packet approaches a rectangular shape. However, if the EIT loss is significant, R_2 follows an exponential decay. The frequencies generated out of the phase-matching spectrum, but remaining within the allowable range of the optical response, leads to a sharp peak in the leading edge of the two-photon (and three-photon) coincidence counts. This sharp peak is a signature of Sommerfeld–Brillouin precursor [51] in the quantum region. The first observed Sommerfeld–Brillouin precursor at the biphoton level has been recently reported in [52].

B. Three-Photon Coincidences

We now turn to look at the three-photon temporal correlation for the experiment diagramed in Fig. 1(a). By applying Eqs. (7) and (23), the three-photon amplitude (21) becomes

$$A_3(\tau_{13},\tau_{23}) = A_{30}\int d\nu_1\chi_1^{(3)} \times(\nu_1)\mathrm{sinc}\left(\frac{\nu_1 L_1}{2v_{as1}}\right)e^{-i\nu_1(\tau_{13}+L_1/2v_{as1})}\int d\nu_2\chi_2^{(3)} \times(\nu_1,\nu_2)\mathrm{sinc}\left(\frac{\nu_2 L_2}{2v_{as2}}\right)e^{-i\nu_2(\tau_{23}+L_2/2v_{as2})}, \quad (30)$$

where all the constants and slowly varying terms have been grouped into A_{30}. The three-photon coincidence counting rate (18) is module squared of A_3. It is easy to show that Eq. (30) is the joint convolution between the third-order susceptibilities and the longitudinal detuning functions. The temporal coherence is determined by the nonlinear susceptibilities and the phase matchings. This sets two simple regions that allow us to gain insight into the underlying physics. The two regions are damped Rabi oscillation regime and group-delay regime, as mentioned in Subsection 3.A. In the following we will consider the triphoton coincidence counts under these two regimes.

Before proceeding with the discussion, we note that by performing conditional three-photon detections, i.e., setting either τ_{13} or τ_{23} as a constant in Eq. (30), the three-photon coincidences yield the same feature as the two-photon coincidences except the rates. In other words, the width of the time correlation in the conditional three-photon measurement is the same as that in the two-photon coincidences.

1. Damped Rabi Oscillation Regime

So, let us first look at the triphoton temporal correlation in the damped Rabi oscillation limit. That is, the pattern of the three-photon temporal coincidences is mainly controlled by the third-order nonlinear susceptibilities. In such a case, the phase matchings may be visualized as poor spectrum (or frequency) filters. The triphoton amplitude (30) then takes a simpler form:

$$A_3(\tau_{13},\tau_{23}) = A_{30}\int d\nu_1\chi_1^{(3)}(\nu_1)e^{-i\nu_1\tau_{13}}\int d\nu_2\chi_2^{(3)}(\nu_1,\nu_2)e^{-i\nu_2\tau_{23}}, \quad (31)$$

which is two-fold Fourier transforms of $\chi_1^{(3)}$ and $\chi_2^{(3)}$. Under the assumption of far detuning of the input ω_{s1} field, Eq. (31) reduces to two independent Fourier transforms. One may notice already that the two-photon coincidences show maximal time-frequency entanglement as biphoton generation in a four-level double-Λ EIT system [32,35], and also share the same feature as the conditional three-photon correlation. The reason is that the involved atomic levels here are real energy levels, not virtual states. These real atomic levels set the allowable frequency tuning for ω_{as1} and ω_{as2} photons. From the energy conserva-

tion, the frequency tuning of the ω_{s2} photon is determined by the sum of those two photons' tuning. Moreover, the far detuning for the input ω_{s1} field releases $\chi_2^{(3)}$ from the dependence on ν_1.

By plugging Eqs. (26) and (27) into Eq. (31), the three-photon coincidence counting rate (18) is ready to be evaluated as,

$$R_3(\tau_{13},\tau_{23}) = R_{30}\prod_{j=1}^{2} e^{-2\gamma_{ej}\tau_{j3}}[1-\cos(\Omega_{ej}\tau_{j3})]\Theta(\tau_{j3}), \quad (32)$$

where R_{30} is a grouped constant. The physics of Eq. (32) is easy to be understood based on the knowledge of paired photon generation from the cold atomic ensembles [25,27–29,32]. The feature of R_3 is a product of the interference between two FWMs occurring in the first EIT system times the interference between two other FWMs in the second system. This also explains why only one interference is clearly observable in the conditional three-photon measurement. By the increasing of γ_{ej} the damped Rabi oscillations shown in triphoton coincidences will be switched to the overdamped Rabi oscillation region. That is, one can suppress the Rabi oscillations down to even less than one complete oscillation period by introducing the fast decay rate. In Fig. 3(a) and 3(b) we have plotted R_3, and both the damped and overdamped Rabi oscillations are obviously observable.

2. Group-Delay Regime

If the temporal coherence of triphotons is mainly determined by phase matching, then we reach the group-delay regime. In such a case, as we have already done in Subsection 3.A.2, the nonlinear susceptibilities in Eq. (30) can be considered as constants. The three-photon amplitude (30) hence reduces to

$$A_3(\tau_{13},\tau_{23}) = A_{30}\int d\nu_1 \mathrm{sinc}\left(\frac{\nu_1 L_1}{2v_{as1}}\right)e^{-i\nu_1(\tau_{13}+L_1/2v_{as1})}\int d\nu_2 \times \mathrm{sinc}\left(\frac{\nu_2 L_2}{2v_{as2}}\right)e^{-i\nu_2(\tau_{23}+L_2/2v_{as2})}. \quad (33)$$

Again, A_{30} has absorbed all the slowly varying terms and constants. In this group-delay region, the three-photon wave packet (33) turns to be two independent Fourier transforms of sinc functions. This also explains why the conditional triphoton coincidences share the similar pattern with two-photon coincidence counts as discussed in Subsection 3.A.2. Fourier transform of a sinc function gives a rectangular function, and the width of the rectangular function is determined by the maximal time delay, L_j/v_{asj}. As mentioned before, in this regime the mechanism of entangled photon generation is washed out due to the longer time coherence from the phase matchings. The frequencies produced out of the phase-matching spectral window but allowed in optical response would contribute to the three-photon precursor phenomena. They will lead to a sharp peak at the leading edge in the coincidences, similar to the observed biphoton precursor [52]. If the EIT loss could not be tolerant, the three-photon correlation will follow exponential decays.

It is worthwhile to mention that if each photon experiences appreciable group delay during the propagation within the materials (e.g., nonlinear crystals), the conditional three-photon correlation may have a narrower width than the two-photon correlation, as shown in [16]. In such a case, only partial entanglement remains between two subsystems in tripartite W states.

Finally for this section, let us look at the suitable atomic level structures for the experiment. Take the cold Rubidium atoms as an example. The first ensemble may choose the ^{87}Rb D_1 transition hyperfine levels for consideration. $|5^2S_{1/2},F=1\rangle$ and $|5^2S_{1/2},F=2\rangle$ are set as two

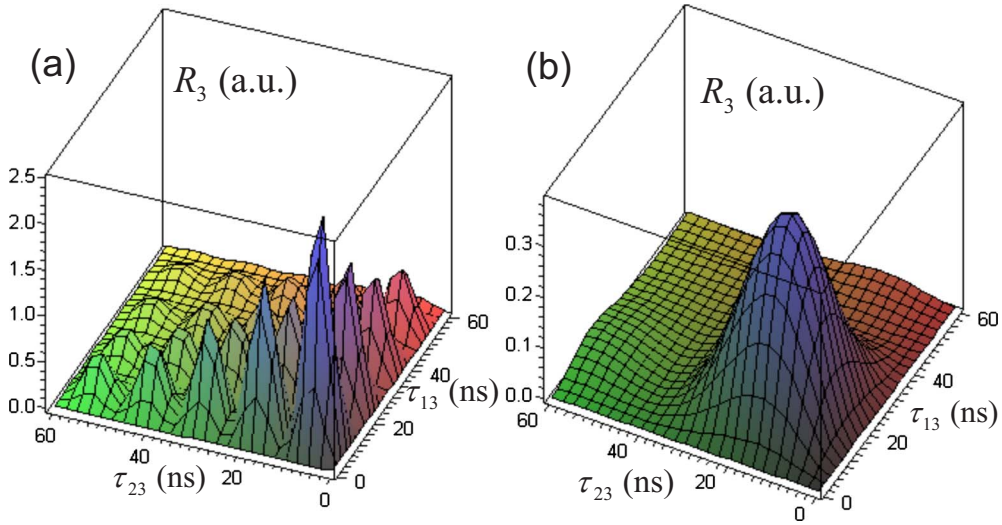

Fig. 3. (Color online) Triphoton coincidences in the damped (a) and overdamped Rabi oscillation regions. The same parameters are chosen as in Figs. 2(b) and 2(b) plus $\Omega_{c2}=28\gamma_{31}$.

ground levels $|1\rangle_1$ and $|2\rangle_2$, and accordingly, $|5^2P_{1/2},F=1\rangle$ and $|5^2P_{1/2},F=2\rangle$ are set as two excitation levels $|4\rangle_1$ and $|3\rangle_1$. The second atomic gas may choose the ^{85}Rb D_1 transition hyperfine levels for the FWM process. $|5^2S_{1/2},F=2\rangle$ and $|5^2S_{1/2},F=3\rangle$ are corresponding to two ground levels $|1\rangle_2$ and $|2\rangle_2$, and $|5^2P_{1/2},F=2\rangle$ and $|5^2P_{1/2},F=3\rangle$ to two excitation levels $|4\rangle_2$ and $|3\rangle_2$, respectively. To increase the nonlinearity, in principle, it would be better to have the input ϖ_{s1} field closer to the transition $|1\rangle_2 \rightarrow |4\rangle_2$.

4. CONCLUSION

In this paper we have proposed a method to generate a three-photon W state entangled in time (and space) using two four-wave mixing processes in two cold atomic ensembles. To enhance the nonlinear interaction, confining cold atoms with hollow fibers or high-Q cavities may provide an excellent environment for these studies. We have adopted second-order perturbation theory to look at the optical property of the three-photon state. To show the (partial) entanglement between two subsystems in such a state, we have studied both two-photon and triphoton coincidence counting rates. Considering the temporal coherence determined by either the nonlinear susceptibilities or the phase matchings, we have concentrated on two regimes, damped Rabi oscillation and group delay, which allow us to get insight into the underlying physics. Since these narrowband triphotons are produced near atomic resonances with the assistance of EIT, they have properties of long time coherence and long coherence length, which make them ideal for long-distance quantum communication and quantum information processing. In principle, the scheme proposed here could be extended to create an N-photon entangled W state in time (and space) [53]. It may be of interest to look at the feasibility of this type of system for the creation of cluster states for the application in quantum computing. Recent research in six-wave mixing using EIT enhancement [54,55] might provide another way to generate triphoton W states in the low light level.

ACKNOWLEDGMENTS

We are grateful to Min Xiao and Morton H. Rubin for helpful discussions. E.O. was supported by the Naval Research Laboratory. S.D. was supported by the Research Grants Council of the Hong Kong Special Administrative Region, China (Project No. HKUST600809).

REFERENCES

1. D. M. Greenberger, M. A. Horne, and A. Zeilinger, "Going beyond Bell's theorem," in *Bell's Theorem, Quantum Theory, and Conceptions of the Universe*, M. Kafatos, ed. (Kluwer, 1989).
2. A. Zeilinger, M. A. Horne, and D. M. Greenberger, NASA Conf. Publ. No. 3135 (National Aeronautics and Space Administration, Code NTT, Washington D.C., 1997).
3. W. Dür, G. Vidal, and J. I. Cirac, "Three qubits can be entangled in two inequivalent ways," Phys. Rev. A **62**, 062314 (2000).
4. A. Cabello, "Bell's theorem with and without inequalities for the three-qubit Greenberger-Horne-Zeilinger and W states," Phys. Rev. A **65**, 032108 (2002).
5. D. Bouwmeester, J.-W. Pan, M. Daniell, H. Weinfurter, and A. Zeilinger, "Observation of three-photon Greenberger-Horne-Zeilinger entanglement," Phys. Rev. Lett. **82**, 1345–1349 (1999).
6. J.-W. Pan, D. Bouwmeester, M. Daniell, H. Weinfurter, and A. Zeilinger, "Experimental test of quantum nonlocality in three-photon Greenberger-Horne-Zeilinger entanglement," Nature **403**, 515–519 (2000).
7. M. Eibl, N. Kiesel, M. Bourennane, C. Kurtsiefer, and H. Weinfurter, "Experimental realization of a three-qubit entangled W state," Phys. Rev. Lett. **92**, 077901 (2004).
8. C. F. Roos, M. Riebe, H. Hänsel, J. Benhelm, G. P. T. Lancaster, C. Becher, F. Schmidt-Kaler, and R. Blatt, "Control and measurement of three-qubit entangled states," Science **304**, 1478–1480 (2004).
9. H. Mikami, Y. Li, K. Fukuoka, and T. Kobayashi, "New high-efficiency source of a three-photon W state and its full characterization using quantum state tomography," Phys. Rev. Lett. **95**, 150404 (2005).
10. Y.-A. Chen, T. Yang, A.-N. Zhang, Z. Zhao, A. Cabello, and J.-W. Pan, "Experimental violation of Bell's inequality beyond Tsirelson's bound," Phys. Rev. Lett. **97**, 170408 (2006).
11. L. K. Shalm, R. B. Adamson, and A. M. Steinberg, "Squeezing and over-squeezing of triphotons," Nature **457**, 67–70 (2009).
12. J. Yang, X.-H. Bao, H. Zhang, S. Chen, C.-Z. Peng, Z.-B. Chen, and J.-W. Pan, "Experimental quantum teleportation and multiphoton entanglement via interfering narrowband photon sources," Phys. Rev. A **80**, 042321 (2009).
13. P. van Loock and S. L. Braunstein, "Multipartite entanglement for continuous variables: A quantum teleportation network," Phys. Rev. Lett. **84**, 3482–3485 (2000).
14. P. Van Loock and S. L. Braunstein, "Greenberger-Horne-Zeilinger nonlocality in phase space," Phys. Rev. A **63**, 022106 (2001).
15. G. Giedke, B. Kraus, M. Lewenstein, and J. I. Cirac, "Separability properties of three-mode Gaussian states," Phys. Rev. A **64**, 052303 (2001).
16. J.-M. Wen and M. H. Rubin, "Distinction of tripartite Greenberger-Horne-Zeilinger and W states entangled in time (or energy) and space," Phys. Rev. A **79**, 025802 (2009).
17. J.-M. Wen, P. Xu, M. H. Rubin, and Y.-H. Shih, "Transverse correlations in tripartite entanglement: Geometrical and physical optics," Phys. Rev. A **76**, 023828 (2007).
18. J.-M. Wen, M. H. Rubin, and Y.-H. Shih, "Spatial resolution enhancement in quantum imaging beyond the diffraction limit using entangled photon-number state," ArXiv:0812.2032.
19. L.-M. Duan, M. D. Lukin, J. I. Cirac, and P. Zoller, "Long-distance quantum communication with atomic ensembles and linear optics," Nature **414**, 413–418 (2001).
20. Y.-H. Shih, "Entangled biphoton source—property and preparation," Rep. Prog. Phys. **66**, 1009–1044 (2003).
21. Z. Y. Ou and Y. J. Lu, "Cavity enhanced spontaneous parametric down-conversion for the prolongation of correlation time between conjugate photons," Phys. Rev. Lett. **83**, 2556–2559 (1999).
22. H. Wang, T. Horikiri, and T. Kobayashi, "Polarization-entangled mode-locked photons from cavity-enhanced spontaneous parametric down-conversion," Phys. Rev. A **70**, 043804 (2004).
23. C. E. Kuklewicz, F. N. C. Wong, and J. H. Shapiro, "Time-bin-modulated biphotons from cavity-enhanced down-conversion," Phys. Rev. Lett. **97**, 223601 (2006).
24. J. S. Neergaard-Nielsen, B. M. Nielsen, H. Takahashi, A. I. Vistnes, and E. S. Polzik, "High purity bright single photon source," Opt. Express **15**, 7940–7949 (2007).
25. J.-M. Wen and M. H. Rubin, "Transverse effects in paired-photon generation via an electromagnetically induced transparency medium. I. Perturbation theory," Phys. Rev. A **74**, 023808 (2006).
26. J.-M. Wen and M. H. Rubin, "Transverse effects in paired-photon generation via an electromagnetically induced

transparency medium. II. Beyond perturbation theory," Phys. Rev. A **74**, 023809 (2006).
27. J.-M. Wen, S. Du, and M. H. Rubin, "Biphoton generation in a two-level atomic ensemble," Phys. Rev. A **75**, 033809 (2007).
28. J.-M. Wen, S. Du, and M. H. Rubin, "Spontaneous parametric down-conversion in a three-level system," Phys. Rev. A **76**, 013825 (2007).
29. J.-M. Wen, S. Du, Y. P. Zhang, M. Xiao, and M. H. Rubin, "Nonclassical light generation via a four-level inverted-Y system," Phys. Rev. A **77**, 033816 (2008).
30. P. Kolchin, "Electromagnetically-induced-transparency-based paired photon generation," Phys. Rev. A **75**, 033814 (2007).
31. C. H. R. Ooi and M. O. Scully, "Two-photon correlation in a cascade amplifier: Propagation effects via a simple model, nonclassical regimes, and validity of neglecting Langevin noise," Phys. Rev. A **76**, 043822 (2007).
32. S. Du, J.-M. Wen, and M. H. Rubin, "Narrowband biphoton generation near atomic resonance," J. Opt. Soc. Am. B **25**, C98–C108 (2008).
33. C. I. Osorio, S. Barreiro, M. W. Mitchell, and J. P. Torres, "Spatial entanglement of paired photons generated in cold atomic ensembles," Phys. Rev. A **78**, 052301 (2008).
34. Y. P. Huang and M. G. Moore, "Ultra-bright biphoton emission from an atomic vapor based on Doppler-free four-wave-mixing and collective emission," arXiv:0901.4789.
35. V. Balić, D. A. Braje, P. Kolchin, G. Y. Yin, and S. E. Harris, "Generation of paired photons with controllable waveforms," Phys. Rev. Lett. **94**, 183601 (2005).
36. P. Kolchin, S. Du, C. Belthangady, G. Y. Yin, and S. E. Harris, "Generation of narrow-bandwidth paired photons: Use of a single driving laser," Phys. Rev. Lett. **97**, 113602 (2006).
37. S. Du, J.-M. Wen, M. H. Rubin, and G. Y. Yin, "Four-wave mixing and biphoton generation in a two-level system," Phys. Rev. Lett. **98**, 053601 (2007).
38. S. Du, P. Kolchin, C. Belthangady, G. Y. Yin, and S. E. Harris, "Subnatural linewidth biphotons with controllable temporal length," Phys. Rev. Lett. **100**, 183603 (2008).
39. H. J. Metcalf and P. van der Straten, *Laser Cooling and Trapping* (Springer-Verlag, 1999).
40. S. E. Harris, "Electromagnetically induced transparency," Phys. Today **50**(7), 36–41 (1997).
41. M. Fleischhauer, A. Imamoglu, and J. Marangos, "Electromagnetically induced transparency: Optics in coherent media," Rev. Mod. Phys. **77**, 633–673 (2005).
42. M. V. Chekhova, O. A. Ivanova, V. Berardi, and A. Garuccio, "Spectral properties of three-photon entangled states generated via three-photon parametric down-conversion in a $\chi^{(3)}$ medium," Phys. Rev. A **72**, 023818 (2005).
43. T. E. Keller, M. H. Rubin, Y.-H. Shih, and L.-A. Wu, "Theory of the three-photon entangled state," Phys. Rev. A **57**, 2076–2079 (1998).
44. M. Bajcsy, S. Hofferberth, V. Balić, T. Peyronel, M. Hafezi, A. S. Zibrov, V. Vuletic, and M. D. Lukin, "Efficient all-optical switching using slow light within a hollow fiber," Phys. Rev. Lett. **102**, 203902 (2009).
45. J. K. Thompson, J. Simon, H. Loh, and V. Vuletic, "A high-brightness source of narrowband, identical-photon pairs," Science **313**, 74–77 (2006).
46. M. H. Rubin, D. N. Klyshko, Y.-H. Shih, and A. V. Sergienko, "Theory of two-photon entanglement in type-II optical parametric down-conversion," Phys. Rev. A **50**, 5122–5133 (1994).
47. D. N. Klyshko, *Photons and Nonlinear Optics* (Gordon and Breach, 1988).
48. L. Mandel and E. Wolf, *Optical Coherence and Quantum Optics* (Cambridge Univ. Press, 1995).
49. M. D. Lukin, P. R. Hemmer, and M. O. Scully, "Resonant nonlinear optics in phase-coherent media," in Adv. At., Mol., Opt. Phys. Vol. 42, B. Bederson and H. Walther, eds. (Elsevier, 2000), pp. 347–386.
50. M. H. Rubin, "Transverse correlation in optical spontaneous parametric down-conversion," Phys. Rev. A **54**, 5349–5360 (1996).
51. L. Brillouin, *Wave Propagation and Group Velocity* (Academic, 1960).
52. S. Du, C. Belthangady, P. Kolchin, G. Y. Yin, and S. E. Harris, "Observation of optical precursors at the biphoton level," Opt. Lett. **33**, 2149–2151 (2008).
53. J.-M. Wen, M. H. Rubin, and Y.-H. Shih, "Transverse correlations in multiphoton entanglement," Phys. Rev. A **76**, 045802 (2007).
54. Y. P. Zhang, A. W. Brown, and M. Xiao, "Opening four-wave mixing and six-wave mixing channels via dual electromagnetically induced transparency windows," Phys. Rev. Lett. **99**, 123603 (2007).
55. Y. P. Zhang, U. Khadka, B. Anderson, and M. Xiao, "Temporal and spatial interference between four-wave mixing and six-wave mixing channels," Phys. Rev. Lett. **102**, 013601 (2009).